NSTIF ERTS- SQT

E83-10183
CR-169837

Final Report

to

NASA Goddard Space Flight Center
Greenbelt, Maryland 20771

on

Crustal Interpretation of the MAGSAT Data in the Continental United States

(Contract Number - NAS5-26157)

submitted by

I.J. Won and K.H. Son
Department of Marine, Earth and Atmospheric Sciences
North Carolina State University
Raleigh, North Carolina 27650

December 1982

(E83-10183) CRUSTAL INTERPRETATION OF THE MAGSAT DATA IN THE CONTINENTAL UNITED STATES Final Report (North Carolina State Univ.) 35 p HC A03/MF A01 CSCL 08G

N83-17993

Unclas
G3/43 00183

Table of Contents

Summary

The MAGSAT scalar data are processed to construct a crustal magnetic anomaly map over the continental U.S. The processing steps include a removal of the reference field model, a path-by-path subtraction of a low order polynomial through a least-squares fit to reduce orbital offset errors, and a two-dimensional spectral filtering to mitigate the spectral bias induced by the path-by-path orbital correction scheme. The resultant anomaly map shows reasonably good correlations with an aeromagnetic map derived from the project MAGNET. Prominent satellite magnetic anomalies are identified in terms of geological provinces and age boundaries.

To reduce the MAGSAT data to a common altitude, we attempted three types of functional representations of the field, namely, a spherical harmonic series, a finite harmonic series, and a triple half-range cosine series. While these representations properly reduce simulated satellite data to a common level, their results derived from the actual MAGSAT data show unacceptably high rms residual errors. This implies that the difference in the magnetic data among different satellite paths cannot be solely accounted for by the variations in orbital altitude alone. Only after the temporal changes in the external field are properly removed, can the data be reduced successfully to a common level.

Finally, we applied to the MAGSAT data a newly developed method of estimating the Curie depth. The inversion method produces both the Curie depth topography and laterally varying magnetic susceptibility of the crust. A contoured Curie depth map thus derived shows general agreements with a crustal thickness map based on seismic data.

Based on the current study, we believe that the satellite magnetometry, particularly with improved methods of correcting the external field variation, can make further significant contributions toward the understanding of the earth's crustal structure.

Analysis of the MAGSAT data over the U.S.

The MAGSAT data used for this report consist of the entire Investigator B data file for the satellite duration. The data area is bounded by latitudes 24N-52N and longitudes 230E-295E. The magnetic field measured at the satellite level consists of various contributions: the internal and external parts of the geomagnetic field, its temporal variations, and the anomalous field caused by magnetized bodies in the crust of the earth. In order to study the crustal contribution of the field, we selected only those geomagnetically quiet time data (geomagnetic planetary index K_p less than 2+) and removed the reference field of MGST (6/80) (Langel et al., 1981).

Figure 1 shows the distribution of data as a function of satellite altitude. We notice that the majority (56%) of the total 49,000 data points fall within the altitude range between 350-450 km. Figure 2 shows spatial distribution over the U.S. of about one third of the total data used for the study. As expected, the data are evenly distributed over the entire region.

The wide scatter of the satellite altitude poses a rather difficult problem of compiling and presenting the data as a single magnetic anomaly map. To demonstrate this problem we show, in Figure 3, a contoured map of the raw data falling in a relatively small altitude window between 350-400 km without any corrections. By limiting the altitude range, we initially attempted to minimize the effect of the altitude variation.

The orginal data were resampled on a 1 x 1 degree grid for contouring. The value at each grid point was evaluated using all data within a circular area of a three-degree radius and imposing a weighting function of 1/R where R is the distance between the grid point and the data point. No reduction of data to a common altitude was made.

The orginal data thus contoured show numerous narrow anomalies parallel to the satellite paths. These anomalies are believed to be caused by differences of the satellite altitude, static bias, and drift rate among paths as well as temporal variations of the external geomagnatic field. In order to reduce these inconsistencies among different paths, we removed a best-fitting low order polynominal along each path, thus minimizing the rms difference between the observed data and the predicted reference field data. The optimum order of the polynomial obviously depends on the linear path length and longest wavelength features desired to be retained. We have tested polynomials of order 0, 1, and 2. Among these, we find, somewhat subjectively, the first order polynominal most optimal. The resultant map, after removing the first order polynomials, is shown on Figure 4. The average slope is found to be 3.5×10^{-3} gamma/km, with a standard deviation of 5.7×10^{-3} gamma/km, implying that the drift rate is highly random among paths (Won and Son, 1982). The removal of a second order polynomial for each path did not change the result significantly and showed signs of over-correction indicated by some diminishing long wavelength anomalies.

The removal of a best-fit polynomial along each flight path reduces considerably the offset problems among adjacent paths, thereby eliminating narrow north-south flight line anomalies. However, since the scheme does not take into consideration the three-dimensional nature of the magnetic field outside the flight paths, it can potentially create spurious long wavelength east-west trending anomalies. Most MAGSAT anomaly maps, including the one shown on Figure 4, manifest dominant east-west trending anomalies while suspiciously lacking north-south trending anomalies. From a mathematical viewpoint, once we remove a 13th order-and-degree reference field, the resultant data should not contain any anomalies whose spatial wavelengths are greater than those of the highest harmonic constituent. The fact that these

long wavelength anomalies still exist leads us to believe that the path-by-path polynomial adjustment is the potential source of these long wavelength east-west anomalies. We attempted to reduce the dominant east-west anomalies by applying a two-dimensional spectral highpass filter with a cutoff wavelength of 16.5 degrees roughly corresponding to the wavelength of 13th order spherical harmonic term. Figure 5 shows the resultant map after the spectral filtering. The map is now fairly compatible with known geological and geophysical features and will be the basis for geological interpretation later in this report.

Analysis of the MAGNET U.S. Aeromagnetic Data

The MAGNET U.S. aeromagnetic survey data, obtained by the U.S. Naval Oceanographic Office and available from the National Geophysical and Solar-Terrestrial Data Center (NGSTD) of NOAA, were collected during 1976 and 1977 at altitudes above ground level of 500–700 m in non-mountainous terrain and 900 -1,000 m in mountainous terrain. The MAGNET file contains some 650,000 measurements at approximately 100 m intervals along the flight path. Spacing between the N-S flight paths is about 1.1 degree in longitude. Since the data density along the path is much higher than the line spacing, we averaged over every 100 data points to reduce the total data amount to about 6,500 points. This gives approximately a 0.1 degree sampling interval along the path.

Initially, we removed a 13th order-and-degree reference field of GSFC(9/80-2) with secular variation. The residual field thus obtained still showed considerably longer wavelengths than those of the 13th order spherical harmonics. Although the reason for this discrepancy is not clear, it is perhaps due to insufficient removal of the non-crustal field. Other reference field models produced varying, yet similar results.

In order to reduce further the remaining long wavelength anomalies from the data, we removed a best-fitting third order polynomial surface from the MAGNET residual data. The resultant data were contoured from 1 x 1 degree gridded data with the same sampling window and weighting function used for the MAGSAT data. The map (Figure 6) thus produced shows a qualitative resemblence to the MAGSAT anomaly map of Figure 5.

Crustal Geological Interpretation of MAGSAT Data

The MAGSAT map (Figure 7) shows mostly broad-scale features that reflect fundamental crustal structures that persist to depths at which the Curie point is reached. Although some upper crustal structures can be delineated on the map, the finer details that can be correlated on standard aeromagnetic maps (Zietz, 1980) are not present. The anomalies on the MAGSAT map must be related to structures that exist in the lower crust and possibly even the upper mantle in some areas.

Northeast Trending Anomalies

Perhaps the most striking feature of the MAGSAT crustal anomaly map is the northeast trend of the major magnetic anomalies (Figure 7). Northeastern trending structures have been described across the entire United States and represent one of the principal crustal fabrics of the craton. Some of these better documented structural features are:

(1) Colorado lineament - a belt of Precambrian faults (Warner, 1978) that cuts across the Colorado Plateau from south of the Grand Canyon and Rocky Mountains into southeastern Wyoming (Figure 7). It is

approximately aligned with the boundary of two distinct Precambrian terrains in Minnesota (Morey and Sims, 1976).

(2) Proterozoic chronologic province boundary that separates 1690-1780 Ma old rocks on the north from 1610-1680 Ma old rocks on the south (Silver, 1968; Silver, et al., 1977). This boundary extends from southwestern Arizona through northern New Mexico into southeastern Colorado.

(3) Shear zones in the western United States (Chapin, et al., 1978) and in the Great Lakes region (LaBerge, 1972; Sims, 1976).

(4) Midcontinent geophysical anomaly that extends from Lake Superior to Nebraska and is considered to be a major crustal rift. It contains Keweenawan basalts and is flanked by elongated basins filled with red sandstones (King and Zietz, 1971).

(5) New York-Alabama lineament which is defined by a series of linear magnetic anomalies and separates provinces with different trending gravity anomalies (King and Zietz, 1978). Zietz (1980) has pointed out that the lineament seems to delineate the northwestern boundary of a seismically active block in the eastern United States.

(6) Seismically active belt that extends from the St. Lawrence River Valley through New Madrid, Missouri (King and Zietz, 1978).

It is clear that northeast-trending structural features form some of the largest and most pervasive disruptions in the crust across much of the United States. They all pass through regions that overlie Precambrian basement rocks at depth and are well inboard of those areas thought to represent suspect terrains. The parallelism of the northeast-trending crustal structures and the major MAGSAT linear anomalies suggests the two are directly related.

Precambrian Terrains

Precambrian terrains also show some correlation with the MAGSAT data. One of the most striking correlations is the apparent coincidence of the southern boundary of Archean gneiss-migmatite basement (Van Schmus and Bickford, 1981) and the magnetic low that sweeps across the midcontinent from Wisconsin to Colorado and then northwestward into Idaho. This boundary is thought to mark the edge of the Archean craton and, therefore, may represent the site of ancient plate tectonic processes.

Another, less convincing, correlation is the approximate coincidences of the southern boundary of the early Proterozoic (1690-1780 Ma old) belt of metasedimentary, metavolcanic, and plutonic rocks that are largely felsic (Van Schmus and Bickford, 1981) and the northern limit of the belt of magnetic highs that extends from Texas to Michigan. There is no agreement as to the tectonic character of this belt of rocks; both plate margin and intracratonic settings have been proposed to explain its origin. Van Schmus and Bickford (1981) argue rather convincingly that the available data indicate the belt represents a continental margin.

Geological Provinces

On a smaller scale, correlations can also be made with certain geological provinces. Some of the more obvious are:

(1) The Northern Rocky Mountains are magnetically high.

(2) The Middle Rocky Mountains are generally low magnetically except for a weak magnetic high that parallels the Front Range.

(3) The Great Basin of the Basin and Range Provinces is characterized by a magnetic low that may be the result of decrease in depth to the Curie point in that region.

Reduction of Satellite Data to a Common Altitude Surface

In order to remove the effect of altitude variation and to adequately preserve broad-scale magnetic anomalies, we next attempt to reduce the data on a common altitude. There are two principal methods: i) equivalent source representation and ii) functional representation.

Mayhew (1979) used the equivalent source techniques where the parameters for regularly-spaced magnetic dipoles are determined in the least-squares sense so that the magnetic field calculated from such a source distribution approximates the observed data. Bhattacharyya (1977) proposed a technique specifically designed for the efficient reduction of satellite data to a common altitude and inclination. From an equivalent magnetic dipole distribution of magnetization at surface, he calculated the magnetic field at any point above the surface utilizing the relationship between the observed values and the spatial gradient of magnetization.

As for the functional representation approach, we have considered a) a spherical harmonic series, b) a finite harmonic series in Cartesian coordinates, and c) a triple half-range cosine series in Cartesian coordinates (Son and Won, 1982).

First we subjected the entire data over the U.S. to a least-squares fit to the surface spherical harmonic series up to 15th order-and-degree. The resultant coefficients are then used to recompute the field at a common altitude of 350 km (Figure 8). The result is rather disappointing: while the resultant map retains the broad features, it is completely devoid of small features of geological interest. The overall rms error amounts to about 5 gammas. Due to reasons to be discussed later, a further increase in the number of terms does not improve the resolution; nor would the reduction of area size resolve small wavelength features.

Next, we consider the finite harmonic series representation. Henderson and Cordell (1971) used this representation combined with the least-squares technique for three dimensional data. Regan (1979) applied it to reducing satellite magnetic data using Cartesian coordinates. We applied this method to the MAGSAT data over a portion of the eastern U.S.

Figure 9 shows a contour map of raw data in the region uncorrected for orbital offset errors. Figure 10 shows an anomaly map recomputed at 400 km altitude by the finite harmonic series representation using 10 terms along each direction (100 coefficients). The overall rms error is still 2.9 gammas unacceptably high.

Finally, we consider a triple half-range cosine series in the Cartesian coordinates to represent the crustal magnetic field T(x,y,z):

$$T(x,y,z) = \sum_{m=0}^{m_o} \sum_{n=0}^{n_o} \sum_{l=0}^{l_o} A_{mnl} \cos \pi m \frac{x}{L_x} \cos \pi n \frac{y}{L_y} \cos \pi l \frac{z}{L_z} \qquad (1)$$

where L_x, L_y, and L_z are the dimensions of an arbitrary rectangular volume occupying the data space. The coefficient A_{mnl} can be found by the method of least-squares. Once these coefficients are determined for the data they may be used to recompute the field at any point inside the volume. The number of terms to be used in the series approximation m_o, n_o, l_o depends on the size of the region to be analyzed and the required spectral resolution of the crustal field. The method has been tested successfully against sets of simulated satellite data due to simple anomalies. Figure 11 shows the resultant anomaly map through the triple half-range cosine series representation using 6 terms along each direction (216 coefficients) in the eastern U.S. region. The overall rms error is 2.4 gammas.

From all three methods and results, we do not note any significant improvements on the anomaly resolution through the reduction to a common

altitude. Let us consider some basic reasons for this apparent failure in the following.

All three representations are the solutions of the Laplace equation in the respective coordinates and, therefore, physically valid. It should be noted, however, that the raw data subjected to these representations were inevitably <u>not</u> corrected for orbital offsets. Thus, if these orbital offsets are truly caused by the altitude variation alone, the methods should have properly reduced the data to a common altitude to the spatial resolution of the highest order base function used for the field representation. However, it is obvious that these results do not show the spatial resolution prescribed by the series representation.

This fact, along with high overall rms errors, testifies that the altitude variation alone cannot completely account for the orbital offsets. It appears that other causes such as the temporal variations of the external field dominate the orbital offsets. Only after these causes are properly accounted for and removed, the representation method can successfully reduce the data to a common altitude. Presently, we do not seem to have solution for this difficult problem.

Interpretation of MAGSAT Data for Crustal Magnetization

The basic objective in relating the magnetic field data with the crustal structure of the earth is to compute the lower depth limit of magnetized masses in the earth's crust. Rocks lose their magnetism at the Curie temperature at which ferrimagnetic rocks become paramagnetic, and their ability to produce detectable magnetization disappears. Thus, the deepest level in the crust containing materials with discernible magnetization is generally interpreted as the depth to the Curie point isotherm.

The Curie point is about 580°C for magnetite. With appropriate titanium substitutions, Buddington and Lindsley (1964) calculated an average Curie point ranging between 520°C and 560°C for rocks in the deep crust. It is generally believed that the amount of geothermal heatflow should correlate with the Curie depth and thus, in turn, to the crustal magnetic field.

Our main goal is, therefore, to determine the bottom shape of the magnetized crust from a magnetic anomaly map. Since the magnetic anomalies attributable to the bottom geometry are usually quite smaller and have much longer wavelengths than those produced by shallow geological variations, the problem is comparable to searching for a needle in a haystack. Early studies include those by Vacquier and Affleck (1941) and Bhattacharyya and Morley (1965). In both cases, each isolated anomaly was filtered and separately interpreted by the empirical graphic method using a vertical-sided prism.

A more sophisticated method was proposed by Bhattacharyya and Leu (1975a and 1975b). Their method requires an extensive initial filtering of the magnetic data in both regional and short wavelength domains. The filtered data is subsequently divided into a large number of blocks. For each block, a two-dimensional spectrum and its moments are computed and compared with a model of an isolated vertical-sided prism within a block in order to locate the corners of the body. The total amount of computation is tremendous since the method requires a two-dimensional Fourier transform for each block. Applying the method to the Yellowstone National Park area, they produced the Curie isotherm map well correlated with the known geothermal area.

Employing a similar technique, Shuey et al. (1977) concluded that it is essentially impossible to determine Curie depth with any resolution at all by fitting a vertical prism to a single anomaly. The Curie depths they derived could be changed by as much as 10 km without violating the observed data.

This conclusion is seemingly in conflict with those of Bhattacharyya and Leu (1975b).

All methods reviewed here are commonly based on the assumption that there exists an isolated magnetic source for each anomaly. Each individual anomaly is assumed to be caused by a single vertical-sided prism (Bhattacharyya and Leu, 1975a, and 1975b) or a truncated vertical cone (Shuey et al., 1977). Such isolated models are apt to generate spurious anomalies due to their unrealistically well-defined corners and vertical surfaces. These spurious anomalies can induce significant errors in either direct-modelling or spectrum calculation.

Rock formations causing long wavelength magnetic anomalies at a depth close to the Curie point are more likely to have a continuous lateral distribution rather than isolated blocks of well-defined geometrical bodies. A realistic model at this depth should manifest a continuous lateral distribution of magnetic materials having variable thicknesses and susceptibilities.

Fluctuations in long wavelength magnetic anomalies can be attributed to lateral variations either in magnetization strength or in Curie depth. These double uncertainties make the task of simultaneously determining both the magnetizations and the Curie depths very difficult, if not impossible. Similar uncertainties apply to many geophysical modelling theories, e.g., a thin magnetic dike for which the anomaly is the same, as long as the product of thickness and susceptibility remains the same. However, it can be shown that the statement is no longer true if the dike has a considerable thickness, for which case both the thickness and the susceptibility can be independently determined from observed data (Won, 1981). The present approach is based on the classical Gauss method for solving non-linear equations (Corbato, 1965;

Johnson, 1969; Won, 1981) coupled with Marquardt's inversion method (Marquardt, 1963) to derive continuous crustal thickness and susceptibility profiles from regional magnetic data (Won, 1982).

Figure 12 shows the model which is used for inverting magnetic data. The model consists of laminated thick vertical prisms having flat top surfaces and linearly-connected inclined bottom surfaces. The magnetic susceptibility below the lower boundary is assumed to be zero so that the bottom geometry represents the Curie isotherm topography. Although data will be confined within the laminated block region, two semi-infinite slabs are added on either side in order to reduce the edge effects of the first and last blocks. The unknown parameters to be determined are the depth (h's) at each nodal point and the magnetic susceptibility (k's) of each prismatic body.

The model is two-dimensional with an arbitrary strike angle with respect to the magnetic north. Since the method uses total field magnetic data, there is no need for reducing the data to the polar anomalies. The magnetic anomaly generated by a single vertical block having a flat top and an inclined bottom can be derived by analytically combining two inclined dikes. By summing up these individual blocks, we can compute the total field for any given set of blocks having variable depths and susceptibilities (Won, 1982).

Techniques for determining unknown parameters of a nonlinear function involve iteratively correcting currently assumed parameters by differential amounts, thereby minimizing the rms error between the theoretical prediction and the observed data. Two predominant techniques of determining the correction amounts are Gauss' method and the gradient, or the steepest-descent method. Marquardt's method combines these methods by controlling the amounts of differential correction to insure both convergence and speed.

Using the geometrical model and the inversion technique thus described, we analyzed a MAGSAT crustal anomaly profile across U.S. continent at latitude 36°N. Figure 13 shows the data profile and the computed profile along with the bottom topography of the magnetized crust and the lateral susceptibility variation. The rms deviation of the model is only 0.19 gammas.

A total of twelve equally-spaced east-west MAGSAT profiles were subjected to this inversion technique and a Curie depth map is constructed (Figure 14). As expected, the magnetized crust is thin in the oceanic regions (less than 30 km) with relatively high magnetic susceptibilities (see Figure 13), while it is very deep over the geologically old Apalachian region. Comparison of this map with the crustal thickness map (Figure 15) compiled by Allenby (1980) from seismic data shows qualitative agreements. We believe that the inversion technique can be improved even further by adopting a three-dimensional crustal magnetization model.

Acknowledgements

This study has been funded by the NASA Goddard Space Flight Center, Greenbelt, Maryland, through contract NAS5-26157. Dr. M. J. Aldrich of Los Alamos National Laboratory, previously with North Carolina State University, contributed the section of geological interpretation of this report.

References

Allenby, R.J., 1980, United States crustal structure and satellite magnetic anomalies, NASA tech. memo. 81990.

Bhattacharyya, B.K., 1977, Reduction and treatment of magnetic anomalies of crustal origin in satellite data, J. Geophys. Res, v. 82, No. 23, p. 3379-3390.

Bhattacharyya, B.K. and Leu, L.K., 1975a, Spectral analysis of gravity and magnetic anomalies due to two-dimensional structures, Geophysics, v. 40, p. 993-1013.

Bhattacharyya, B.K., and Leu, L.K., 1975b, Analysis of magnetic anomalies over yellowstone National Park: Mapping of Curie point isothermal surface for geothermal reconnaissance, J. Geophys. Res., v. 80, No. 32, p. 4461-4465.

Bhattacharyya, B.K., Moreley, L.W., 1965, The lineation of deep crustal magnetic bodies from total field aeromagnetic anomalies, J. Geomag. Geoelect., v. 17, . 237-252.

Buddington, A.F., and Lindsley, D.H., 1964, Iron-titanium oxide minerals and and synthetic equivalents: J. Petrology, v. 6, p. 310-357.

Carbato, C.E., 1965, A least-squares procedure for gravity interpretation, Geophysics, v. 30, p. 228-233.

Chapin, C.E., Chamberline, R.M., Osburn, G.R., White, D.W., and Sanford, A.R., 1978, Exploration framework of the Socorro geothermal area, New Mexico, in C.E. Chapin and W.E. Elston, editors, Field guide to selected cauldrons and mining districts of the Datil-Mogollon volcanic field, New Mexico. New Mexico Geological Society Special Publications 7, p. 114-129.

Henderson, R.G., and Cordell, L., 1971, Reduction of unevenly spaced potential field data to a horizontal plane by means of finite harmonic series, Geophysics, v. 36, p. 856-866.

Johnson, W.W., 1969, A least-squares method of interpreting magnetic anomalies caused by two-dimensional structures, Geophysics., v. 34, p. 65-74.

King, E.R. and Zietz, I., 1971, Aeromagnetic study of the midcontinent gravity high of central United States. Geological Society of America Bulletin, v. 82, p. 2187-2208.

_________, 1978, The New York-Alabama lineament: geophysical evidence for a major crustal break in the basement beneath the Appalachian basin. Geology, v. 6, p. 312-318.

LaBerge, G.L., 1972, Lineaments and mylonite zones in the Precambrian of northern Wisconsin (abs.). Geological Society of America Abstracts with Programs, v. 4, p. 332.

Langel, R., Berbert, J., Jennings, T., and Horner, R., 1981, MAGSAT data processing: A report for investigators, NASA tech. memo. 82160.

Marquardt, D.V., 1963, An algorithm for least-squares estimation of nonlinear parameters, J. Soc. Indust. Appl. Math., v. 11, No. 2, p. 431-441.

Mayhew, M.A., 1979, Inversion of satellite magnetic anomaly data, J. Geophys., v. 45, p. 119-128.

Morey, G.B. and Sims, P.K., 1976, Boundary between two Precambrian W. terrains in Minnesota and its geologic significance. Geological Society of America Bulletin, v. 87, p. 141-152.

Regan, R.D., 1979, The reduction and analysis of Satellite magnetameter data, Geophysical Survey, v. 3, p. 331-349.

Shuey, R.T., Schellinger, D.K., Tripp, A.C., and Alley, L.B., 1977, Curie depth determination from aeromagnetic spectra, Geophys. J. Roy. Astron. Soc., v. 50, p. 75-101.

Silver, L.T., 1968, Precambrian batholiths of Arizona (abs.) Geological Society of America Special Paper 121, Abstracts for 1968, p. 558-559.

Silver, L.T., Anderson, C.A., Crittenden, M., and Robertson, J.M., 1977, Chronostratigraphic elements of the Precambrian rocks of the southwestern and far western United States (abs.). Geological Society of America, Abstracts with Programs, v. 9, p. 1176.

Sims, P.K., 1976, Precambrian tectonics and mineral deposits, Lake Superior region. Economic Geology, v. 71, p. 1092-1118.

Son, K.H. and Won, I.J., 1982, Crustal interpretation of MAGSAT data over the continental U.S., Presented at 52nd Soc. Exploration Geophysicists Meeting, Dallas, Extended Abstract p. 410-411.

Vacquier, V., Affleck, J., 1941, A computation of the average depth to the bottom of the earth's magnetic crust based on a statistical study of local magnetic anomalies, Trans., Am. Geophys. Union, p. 446-450.

Van Schmus, W.R. and Bickford, M.E., 1981, Proterozoic chronology and evolution of the midcontinent region, North America, in A. Kroner, ed., Precambrian plate tectonics, Elsevier, New York,.

Warner, L.A., 1978, The Colorado lineament: a middle Precambrian wrench fault system. Geological Society of America Bulletin, v. 89, p. 161-171.

Won, I.J., 1981, Application of Gauss' method to magnetic anomalies of dipping dikes, Geophysics, v. 46, p. 211-215.

Won, I.J., and Son, K.H., 1982, A preliminary comparison of the MAGSAT data and aeromagnetic data in the continental U. S., Geoph. Res. Letters, v. 9, no. 4, p. 296-298.

Won, I.J., 1982, Determination of Curie depth from aeromagnetic data, presented at the Hot Dry Rock Geothermal Exploration Symposium at Los Alamos National Lab, June.

Zietz, I., 1980, Exploration of the continental crust using aeromagnetic data, in Studies in Geophysics, National Academy of Sciences, p. 127-138.

Figure Captions

Figure 1. MAGSAT scalar data population as a function of satellite altitude over the continental U.S.

Figure 2. Footprints of one-third of MAGSAT data in the continental U.S.

Figure 3. MAGSAT raw residual data within an altitude window of 350-400 km contoured at a two gamma interval.

Figure 4. MAGSAT anomaly map after removing a best-fit straight line from each path.

Figure 5. MAGSAT anomaly map after a two-dimensional highpass spectral filtering for wavelengths shorter than 16.5 degrees.

Figure 6. MAGNET U.S. aeromagnetic map referenced to GSFC (9/80-2) field model contoured at a 50 gamma interval (after Won and Son, 1982).

Figure 7. Geological correlation of the filtered MAGSAT crustal anomaly map.

Figure 8. Reduction of MAGSAT data to 350 km altitude by a spherical harmonic analysis contoured at a two gamma interval.

Figure 9. MAGSAT raw data over a portion of the eastern U.S contoured at a two gamma interval.

Figure 10. An anomaly map of the eastern U.S. reduced to 400 km altitude through the finite harmonic series representation.

Figure 11. An anomaly map of the eastern U.S. reduced to 400 km altitude through the half-range cosine series representation.

Figure 12. Model geometry used for inversion of magnetic data to estimate the Curie depth and lateral susceptibility variation.

Figure 13. Profiles of the bottom of the magnetized crust and susceptibility based on a MAGSAT crustal anomaly profile at 36°N across the continental U.S.

Figure 14. Thickness of the magnetized crust based in the continental U.S. on the MAGSAT data.

Figure 15. Crustal thickness based on seismic studies (from Allenby, 1980).

ORIGINAL PAGE IS
OF POOR QUALITY

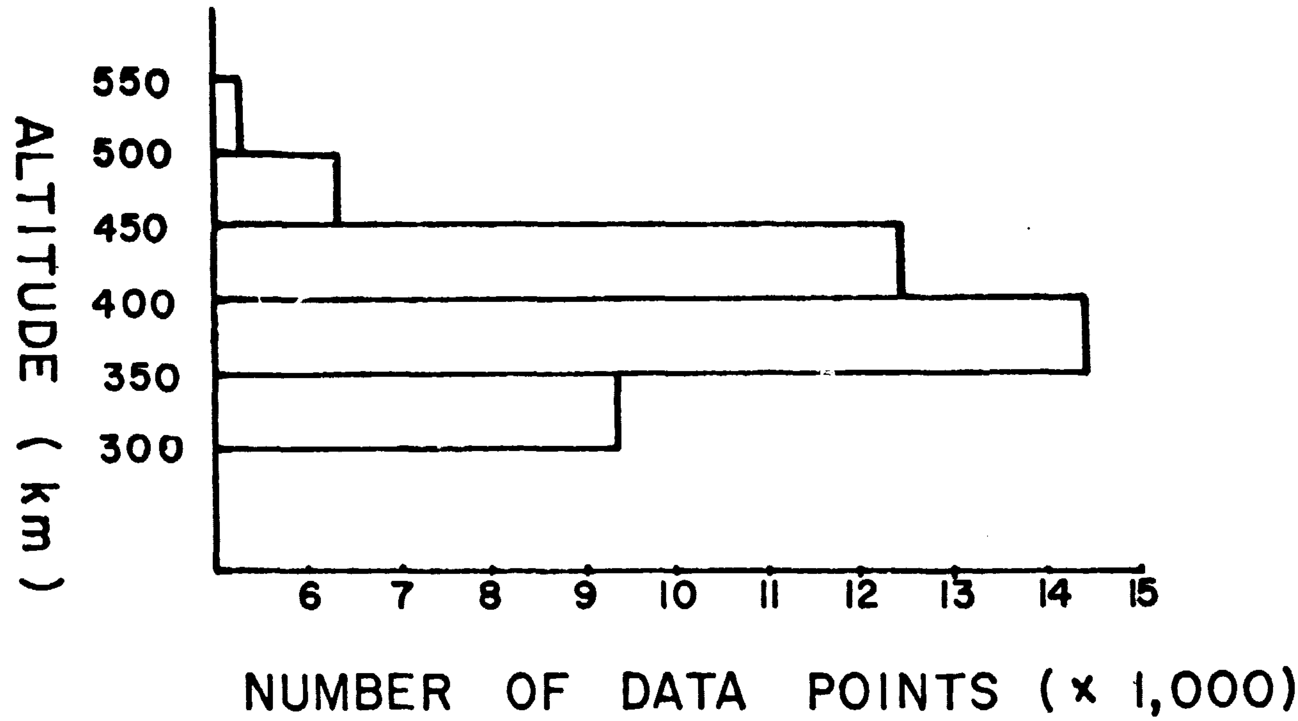

Figure 1. MAGSAT scalar data population as a function of satellite altitude over the continental U.S.

MAGSAT DATA POINTS (11/1/79 - 5/26/80, Kp<2)

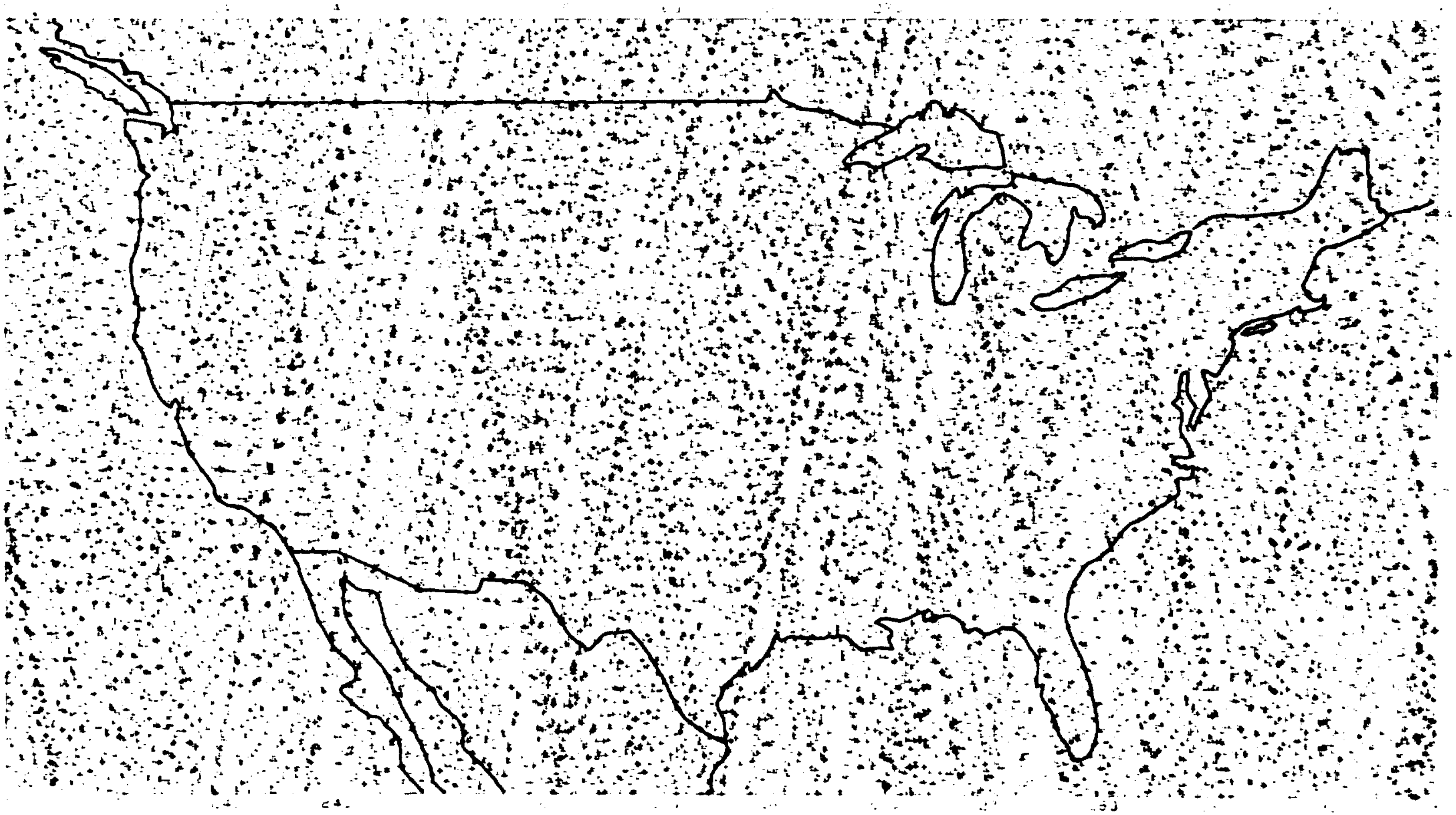

Figure 2. Footprints of one-third of MAGSAT data in the continental U.S.

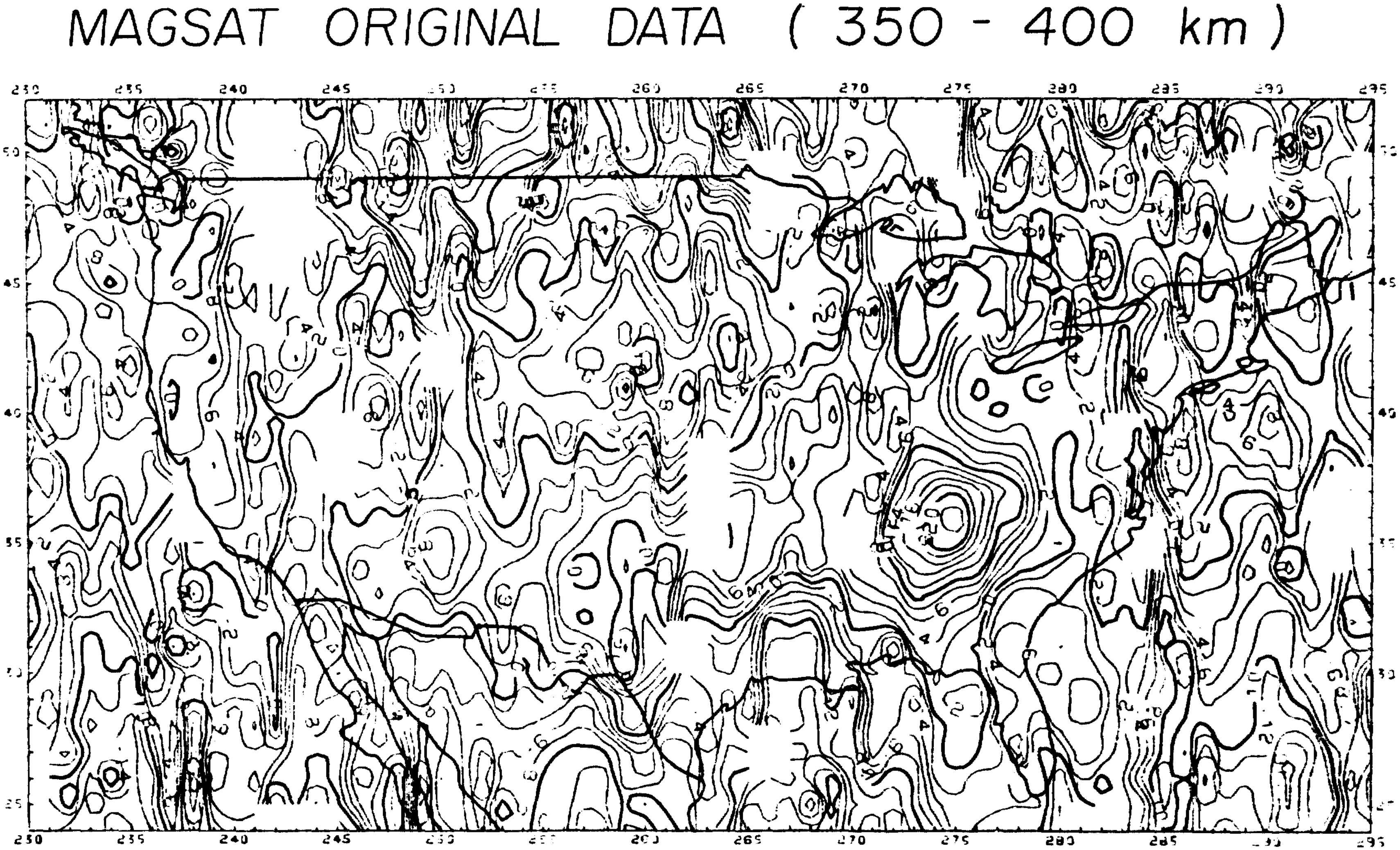

Figure 3. **MAGSAT raw residual data within an altitude window of 350-400 km contoured at a two gamma interval.**

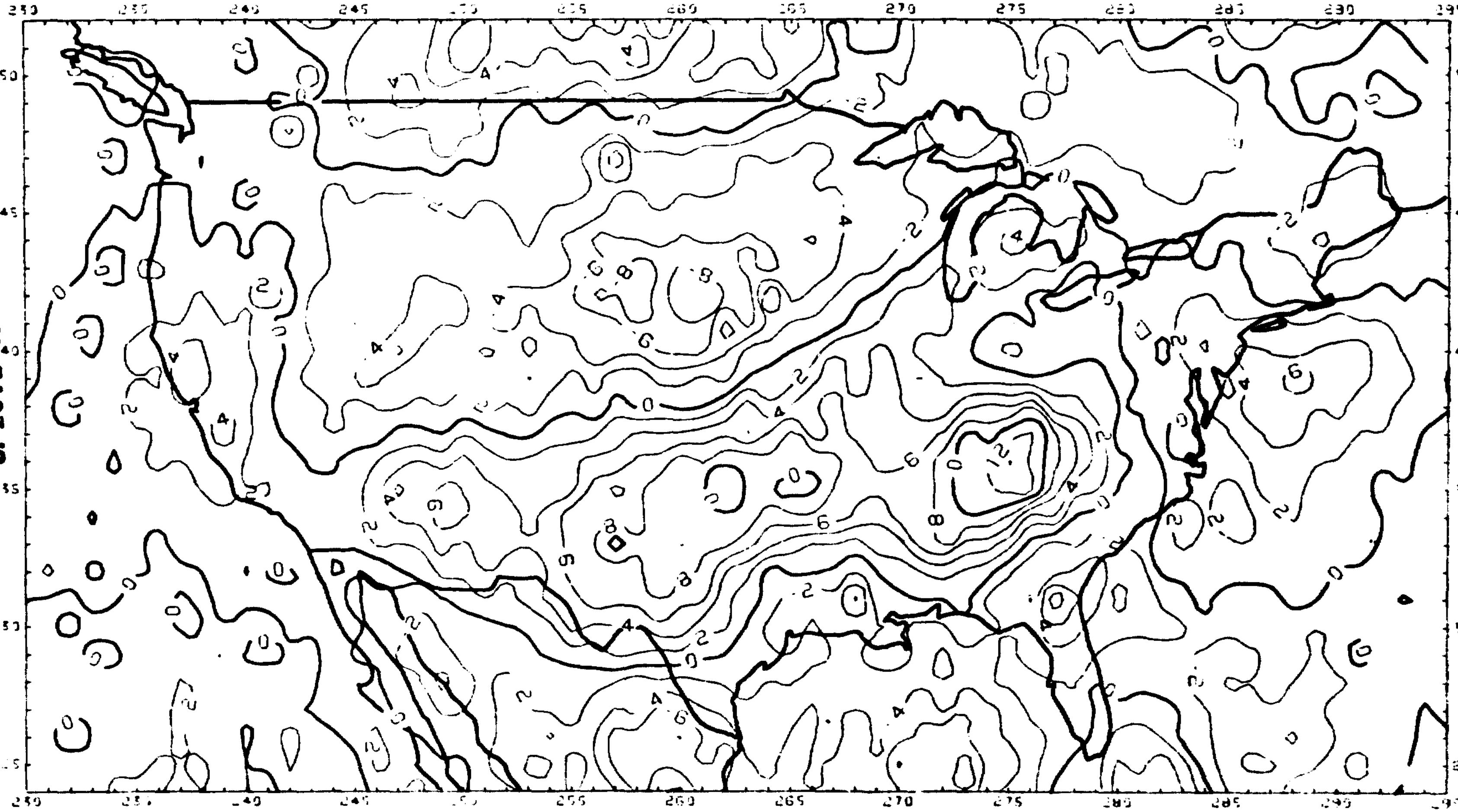

Figure 4. MAGSAT anomaly map after removing a best-fit straight line from each path.

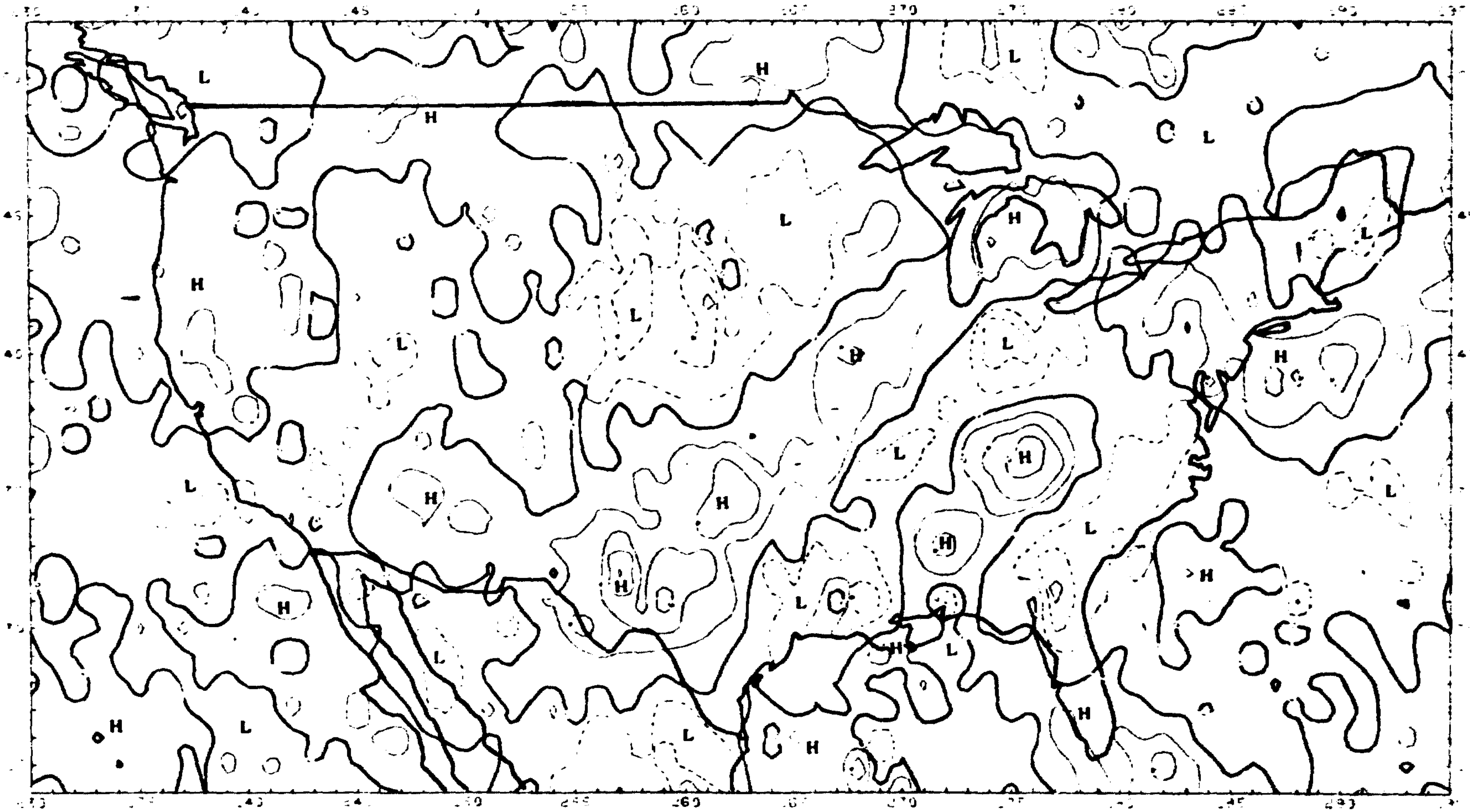

Figure 5. MAGSAT anomaly map after a two-dimensional highpass spectral filtering for wavelengths shorter than 16.5 degrees.

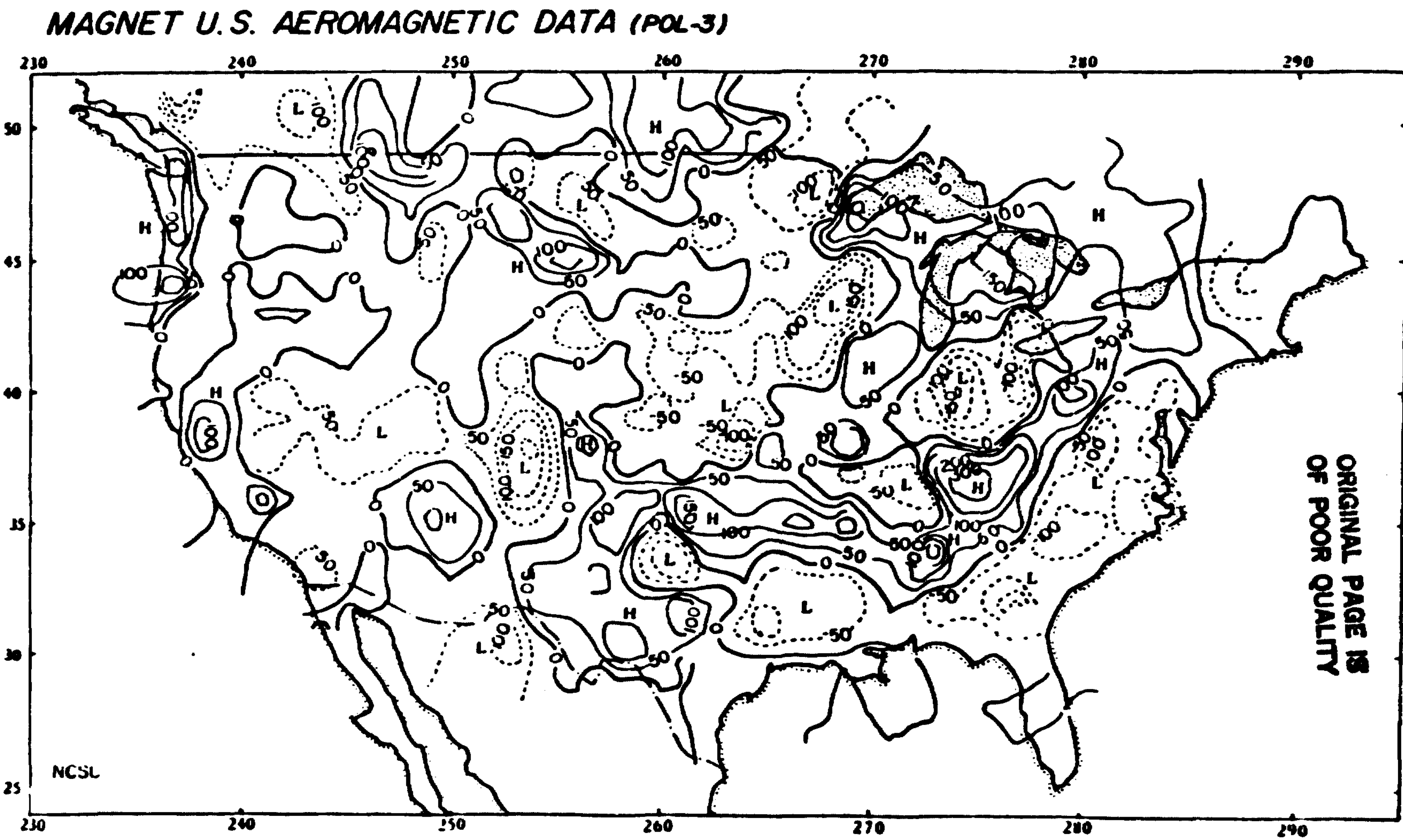

Figure 6. MAGNET U.S. aeromagnetic map referenced to GSFC (9/80-2) field model contoured at a 50 gamma interval (after Won and Son, 1982).

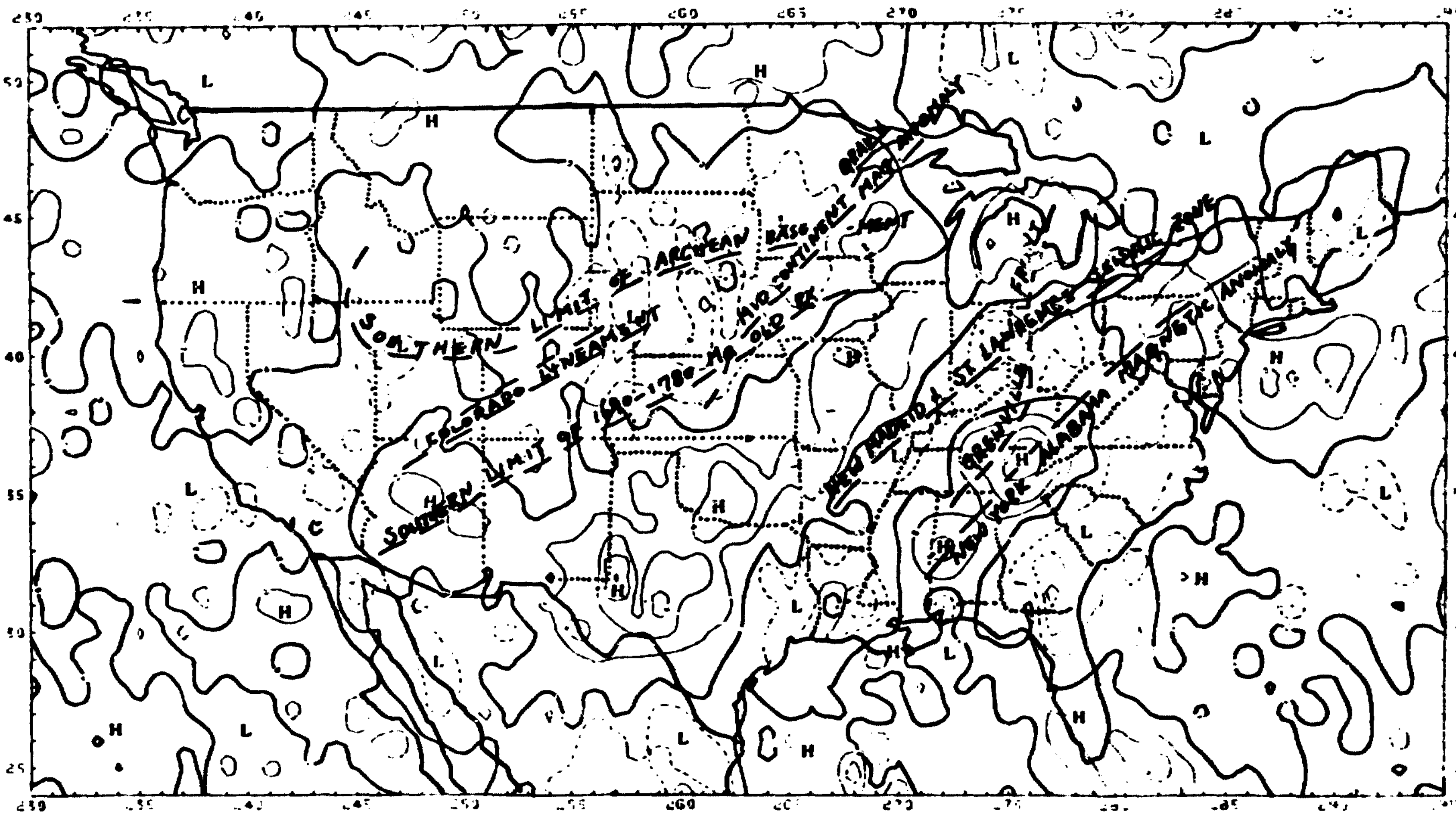

Figure 7. Geological correlation of the filtered MAGSAT crustal anomaly map.

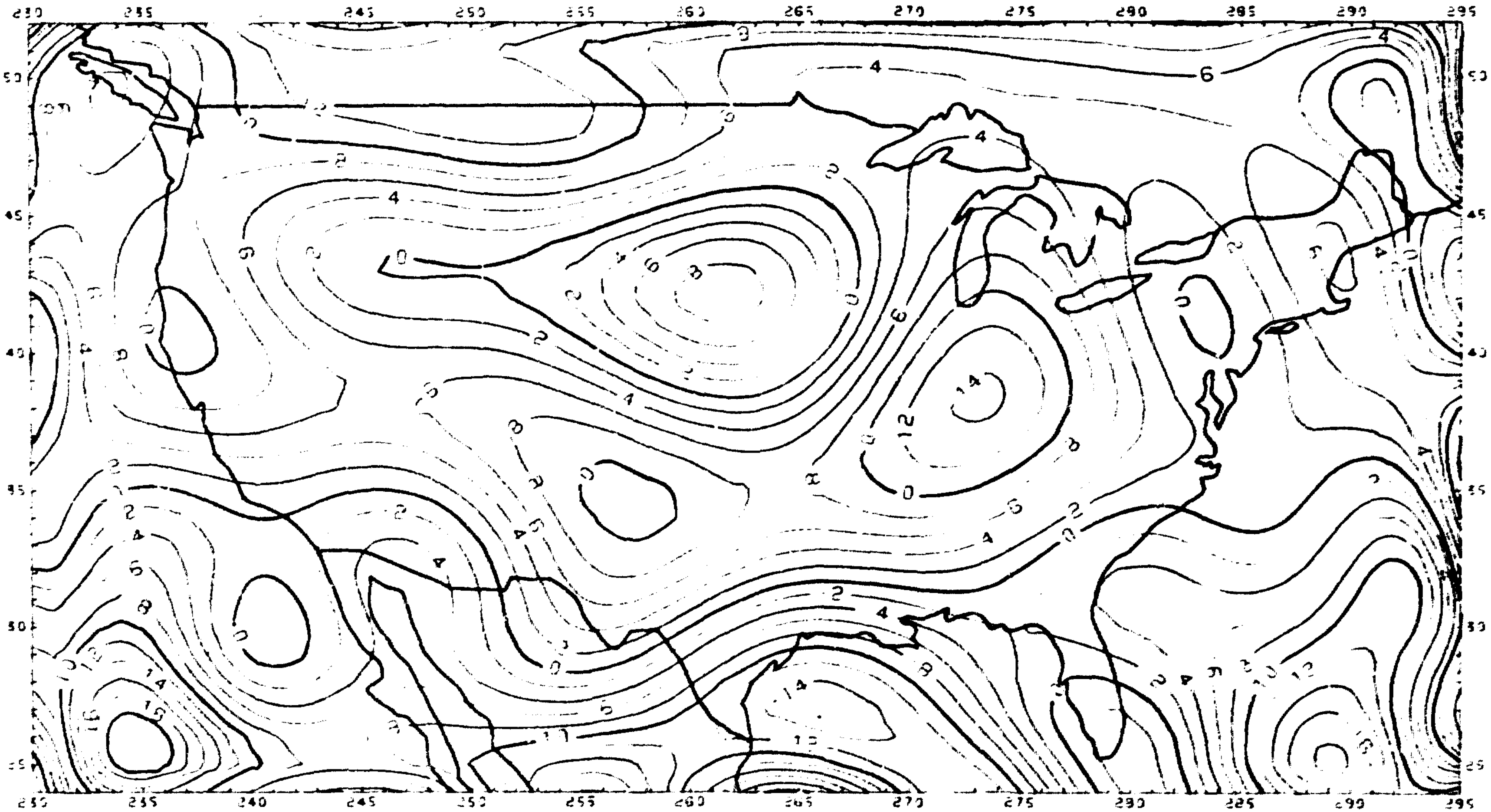

Figure 8. Reduction of MAGSAT data to 350 km altitude by a spherical harmonic analysis contoured at a two gamma interval.

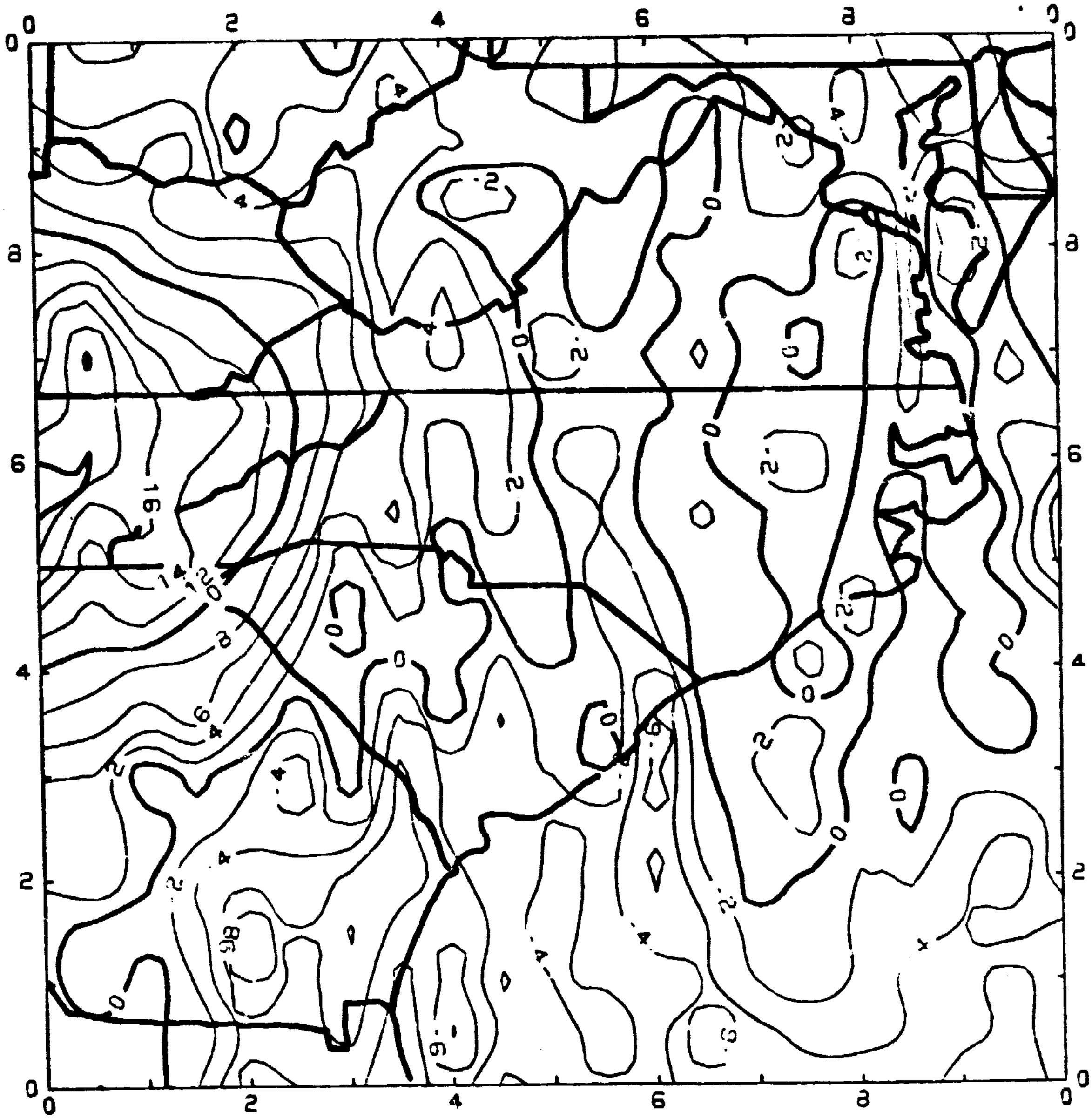

Figure 9. MAGSAT raw data over a portion of the eastern U.S contoured at a two gamma interval.

ORIGINAL PAGE IS
OF POOR QUALITY

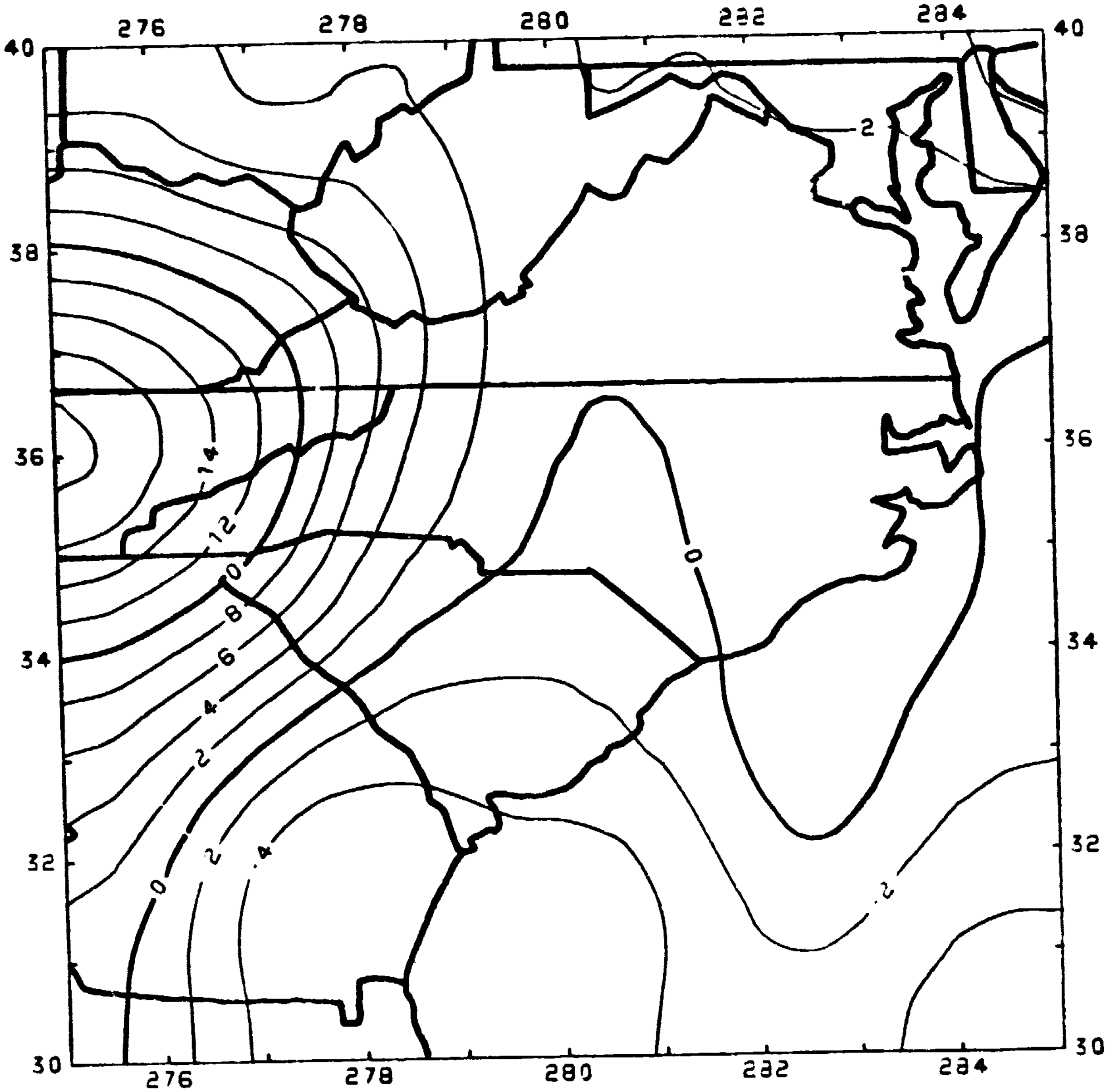

Figure 10. An anomaly map of the eastern U.S. reduced to 400 km altitude through the finite harmonic series representation.

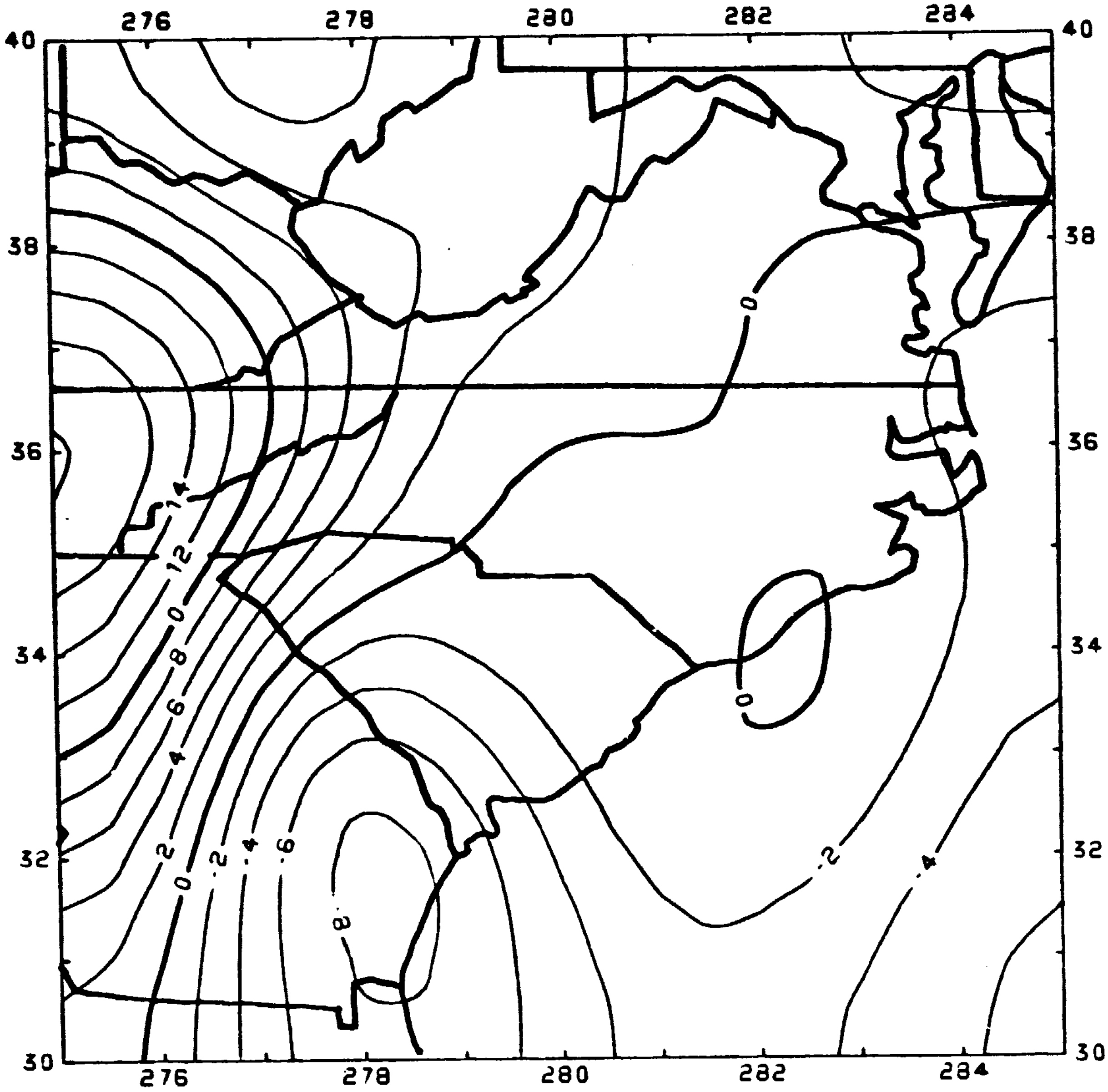

Figure 11. An anomaly map of the eastern U.S. reduced to 400 km altitude through the half-range cosine series representation.

ORIGINAL PAGE IS
OF POOR QUALITY

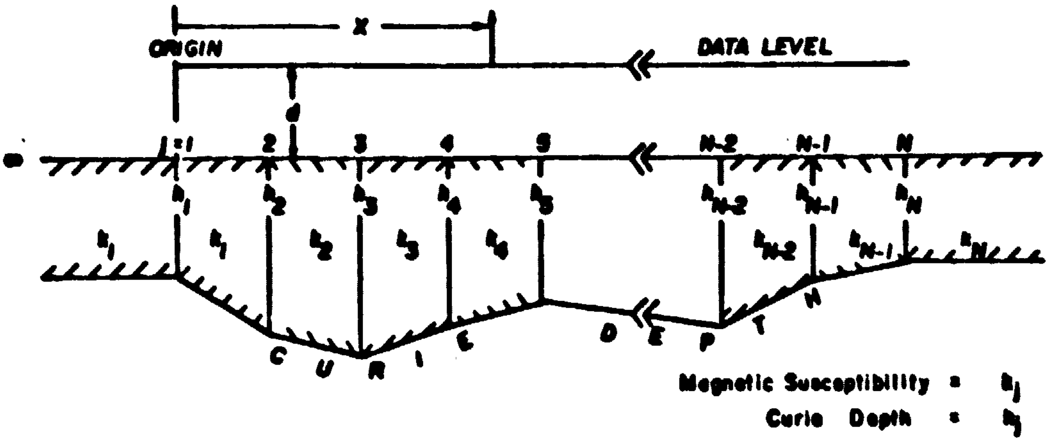

Figure 12. Model geometry used for inversion of magnetic data to estimate the Curie depth and lateral susceptibility variation.

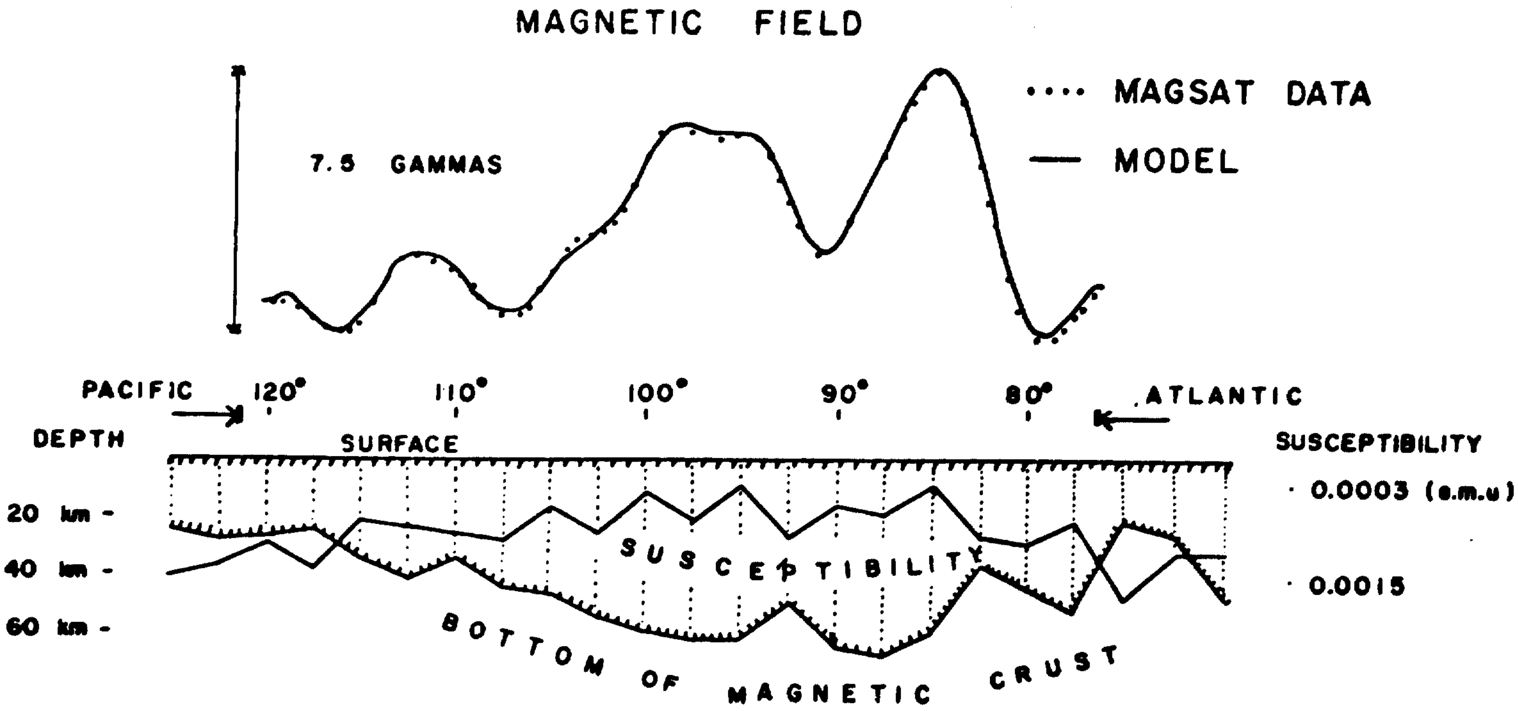

Figure 13. Profiles of the bottom of the magnetized crust and susceptibility based on a MAGSAT crustal anomaly profile at 36°N across the continental U.S.

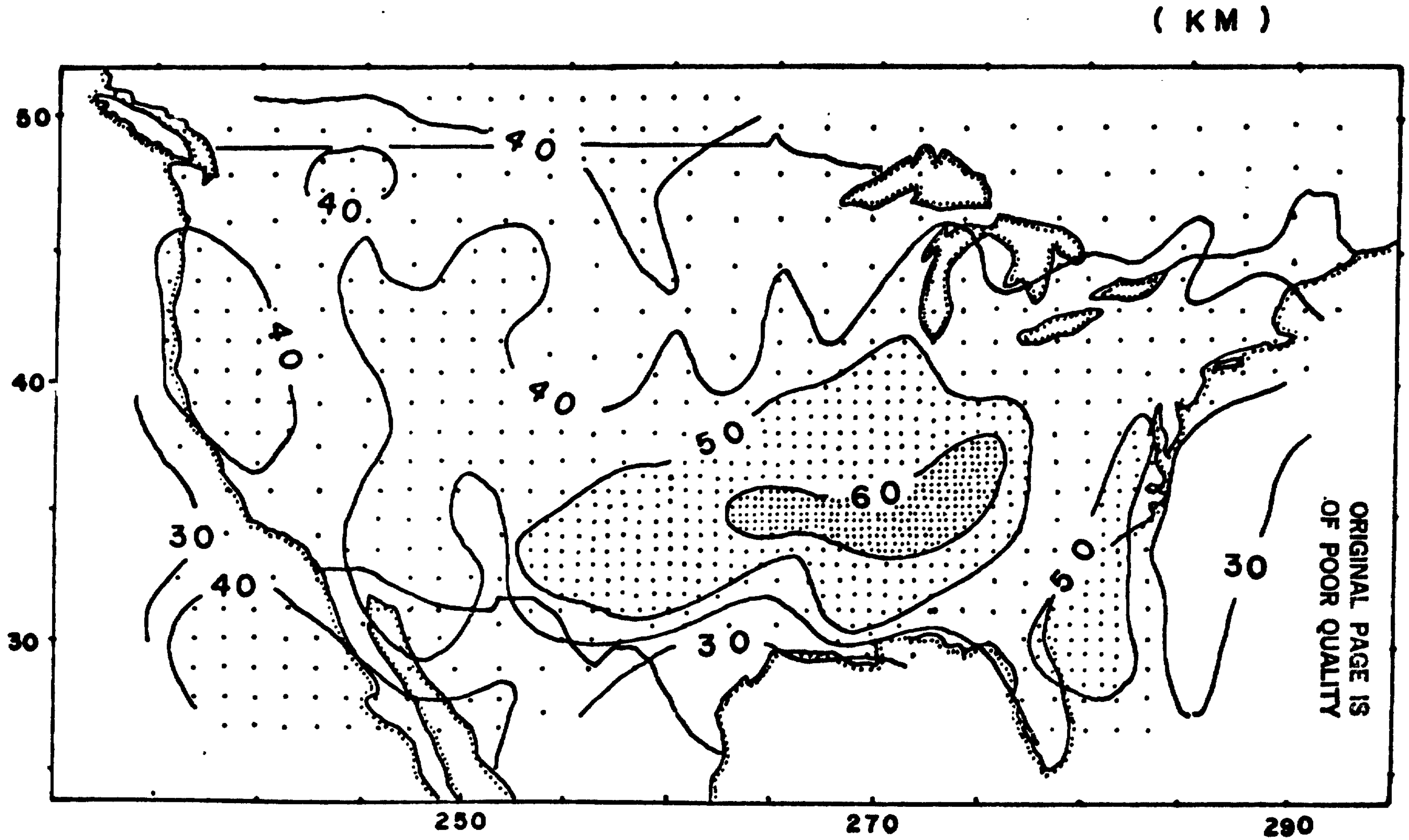

Figure 14. Thickness of the magnetized crust based in the continental U.S. on the MAGSAT data.

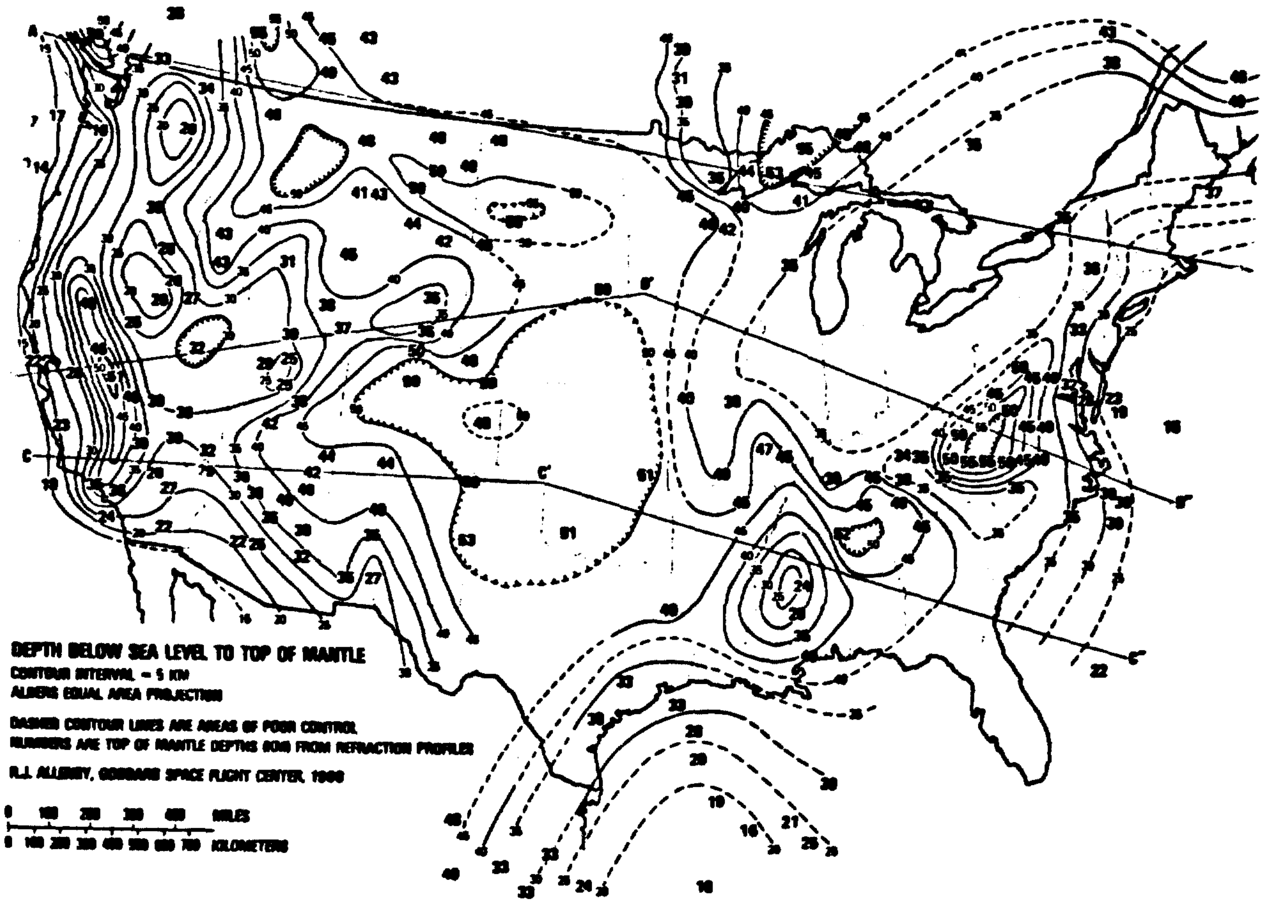

Figure 15. Crustal thickness based on seismic studies (from Allenby, 1980).